Band 4 (22). R_f 0.38. obtained (20 mg; 11% yield) as a purple solid. Small portion recrystallized from $CHCl_3$/methanol, giving small red needles. Mp: >300 °C. Vis: 404 nm (ϵ 43 800), 588 (35 300). NMR (360 MHz): see Table II for chemical shift assignments. Anal. Calcd for $C_{33}H_{36}N_4NiO_3$: C, 66.57; H, 6.09; N, 9.41. Found: C, 66.78; H, 5.68; N, 9.48. MS (FAB positive ion, thioglycerol matrix): 595 [22.2, $(M + H)^+$], 594 (23.6, M^+), 563 (37.4, $M^+ - OMe$), 181 (100, bp, thioglycerol).

Band 5 (23). R_f 0.30. obtained (10 mg; 5% yield) as an orange solid. Vis (Figure 2): 298 nm (ϵ 17 600); 426 (7800), 532 (29 000). NMR (360 MHz): see Figure 2 for spectra and Table I for chemical shift assignments. MS (FAB positive ion, thioglycerol matrix): 599 [100, $(M + H)^+$], 583 (7.2), 567 (22.0, $M^+ - OMe$), 539 (8.8, $M^+ - CO_2Me$).

Acknowledgment. This research was supported by a grant from the National Science Foundation (CHE-81-20891).

Spontaneous and Olefin-Promoted Reductive Elimination of η^3-Allyl(organo)palladium(II) Complexes: Mechanistic and Molecular Orbital Analysis

Hideo Kurosawa,*[1a] Mitsuhiro Emoto,[1a] Hiroaki Ohnishi,[1a] Kunio Miki,[1a] Nobutami Kasai,[1a] Kazuyuki Tatsumi,[1b] and Akira Nakamura[1b]

Contribution from the Department of Applied Chemistry, Osaka University, Suita, Osaka 565, Japan, and the Department of Macromolecular Science, Osaka University, Toyonaka, Osaka 560, Japan. *Received March 11, 1987*

Abstract: Kinetic studies are reported on spontaneous and olefin-promoted reductive elimination of complexes of Pd(η^3-allyl)(Ar)(L) (**1**: Ar = $C_6H_3Cl_2$-2,5; L = PR_3, AsR_3), which affords high yields of the coupling products, allylbenzene derivatives. The rate of the spontaneous process was not affected by addition of free ligands, L, suggesting no significant participation of a η^1-allylpalladium species nor of a 14-electron intermediate arising from ligand dissociation during the C–C bond-forming step. Reductive elimination of structurally rigid Pd(η^1-allyl)(Ar)(dppe) proceeded more slowly than that of **1**. The rate of the olefin-promoted process for **1** (L = AsR_3) showed first-order dependence on the concentration of olefins and inverse dependence on that of AsR_3. A reaction scheme consistent with this observation has been proposed which involves initial ligand exchange between AsR_3 of **1** and olefins to form an intermediate, Pd(η^3-allyl)(Ar)(olefin), followed by the C–C coupling step. These types of olefin complexes for Ar = C_6HCl_4-2,3,5,6 were generated separately in solution at low temperature and characterized by ^1H NMR spectra. Reactivity patterns of the reductive elimination of these olefin complexes unambiguously confirmed the kinetically implicated trend described above, namely they are by far more reactive than the corresponding $AsPh_3$ complex, and the complex having the more electron-withdrawing olefin gives the coupling product more rapidly. Extended Hückel molecular orbital calculations on Pd(η^3-CH_2CHCH_2)(CH_3)L (L = PH_3, $CH_2{=}CH_2$) and related species have been carried out. The MO analyses satisfactorily explain the origin of the above-mentioned reactivity patterns, which are apparently specific to the η^3-allyl complexes.

η^3-Allyl complexes of transition metals are important reagents and intermediates in many organic transformations.[2-5] Recently, increasing attention has been paid to the synthetic value of reductive elimination of η^3-allylmetal complexes.[3-5] Nevertheless, mechanistic studies of this process are scarce aside from some stereochemical examinations,[6] in contrast to remarkable progress concerning mechanistic understanding of the reductive elimination of those complexes that contain only η^1-bound alkyl and aryl ligands.[7-9] However, knowledge in the latter field cannot always be transferable to the η^3-allylmetal chemistry, for the intrinsic difference between the nature of the η^3-allyl–metal and the η^1-alkyl–metal bond may lead to a considerable difference in reactivity patterns of two classes of complexes. Well-known examples include the attack of certain nucleophiles at the metal-bound η^3-allyl ligand from the anti side,[2] whereas very few equivalents of this step are found in the chemistry of the η^1-alkyl complexes.

(1) (a) Department of Applied Chemistry. (b) Department of Macromolecular Science.

(2) (a) Collman, J. P.; Hegedus, L. S. *Principles and Applications of Organotransition Metal Chemistry*; University Science Books: Mill Valley, CA, 1980; p 673. (b) Trost, B. M. *Acc. Chem. Res.* **1980**, *13*, 385. (c) Tsuji, J. *Organic Synthesis with Palladium Compounds*; Springer-Verlag: New York, 1980.

(3) (a) Goliaszewski, A.; Schwartz, J. *Organometallics* **1985**, *4*, 415. (b) Goliaszewski, A.; Schwartz, J. *Ibid.* **1985**, *4*, 417. (c) Goliaszewski, A.; Schwartz, J. *Tetrahedron* **1985**, *41*, 5779. (d) Goliaszewski, A.; Schwartz, J. *J. Am. Chem. Soc.* **1984**, *106*, 5028. (e) Temple, J. S.; Riediker, M.; Schwartz, J. *Ibid.* **1982**, *104*, 1310. (f) Hayasi, Y.; Riediker, M.; Temple, J. S.; Schwartz, J. *Tetrahedron Lett.* **1981**, *22*, 2629.

(4) (a) Hiyama, T.; Wakasa, N. *Tetrahedron Lett.* **1985**, *26*, 3259. (b) Trost, B. M.; Herndon, J. W. *J. Am. Chem. Soc.* **1984**, *106*, 6835. (c) Sheffy, F. K.; Godschalx, J. P.; Stille, J. K. *Ibid.* **1984**, *106*, 4833. (d) Consiglio, G.; Morandini, F.; Piccolo, O. *J. Chem. Soc., Chem. Commun.* **1983**, 112. (e) Matsushita, H.; Negishi, E. *J. Am. Chem. Soc.* **1981**, *103*, 2882. (f) Hayashi, T.; Konishi, M.; Yokota, K.; Kumada, M. *J. Chem. Soc., Chem. Commun.* **1981**, 313. (g) Cherest, M.; Felkin, H.; Umpleby, J. D.; Davies, S. G. *Ibid.* **1981**, 681.

(5) Keim, W.; Behr, A.; Roper, M. *Comprehensive Organometallic Chemistry*; Wilkinson, G., Stone, F. G. A., Abel, E. W., Eds.; Pergamon: Oxford, 1982; Chapter 52.

(6) (a) Hayashi, T.; Konishi, M.; Kumada, M. *J. Chem. Soc., Chem. Commun.* **1984**, 107. (b) Consiglio, G.; Morandini, F.; Piccolo, O. *J. Am. Chem. Soc.* **1981**, *103*, 1846.

(7) (a) Moravskiy, A.; Stille, J. K. *J. Am. Chem. Soc.* **1981**, *103*, 4182. (b) Ozawa, F.; Ito, T.; Nakamura, Y.; Yamamoto, A. *Bull. Chem. Soc. Jpn.* **1981**, *54*, 1868. (c) Tatsumi, K.; Hoffmann, R.; Yamamoto, A.; Stille, J. K. *Ibid.* **1981**, *54*, 1857. (d) Gillie, A.; Stille, J. K. *J. Am. Chem. Soc.* **1980**, *102*, 4933.

(8) (a) Yamamoto, T.; Yamamoto, A.; Ikeda, S. *J. Am. Chem. Soc.* **1971**, *93*, 3350. (b) Morrell, D. G.; Kochi, J. K. *Ibid.* **1975**, *97*, 7262. (c) Tatsumi, K.; Nakamura, A.; Komiya, S.; Yamamoto, A.; Yamamoto, T. *Ibid.* **1984**, *106*, 8181. (d) Komiya, S.; Albright, T. A.; Hoffmann, R.; Kochi, J. K. *Ibid.* **1976**, *98*, 7255. (e) Braterman, P. S.; Cross, R. J.; Young, G. B. *J. Chem. Soc., Dalton Trans.* **1977**, 1892.

(9) Åkermark, B.; Ljungquist, A. *J. Organomet. Chem.* **1979**, *182*, 59.

0002-7863/87/1509-6333$01.50/0

We thought the following problems were especially important in the reductive elimination of the η^3-allyl complexes. (1) What is the type of intermediate, η^1- or η^3-allyl species, that is really participating in the C–C bond formation step? This is of particular importance, since η^3-allylmetal complexes are very prone to undergo η^3- to η^1-allyl interconversion[10] and it has strong bearing on the asymmetric synthesis;[4g] namely, the identity of the diastereo- or enantio-face of the η^3-allyl ligand is lost during such interconversion. (2) How does the electronic property of the ligand affect the barrier to the reductive elimination of the intermediate, be it in the η^3- or η^1-allyl form? The ligand may exert its electronic effect exactly at the C–C bond formation step or it may sometimes do so before this step is reached, as exemplified by crucial ligand dissociation to form a three-coordinate intermediate during the reductive elimination of PdR_2L_2.[7a-c]

There has arisen an indication that the ligand electronic effect is especially important in the reductive elimination of the η^3-allyl complexes. In previous papers[11,12] we showed that the concerted, cis C–C coupling in η^3-allyl(aryl)palladium complexes of type **1** is accelerated by the addition of electron-withdrawing olefins. This methodology of employing olefinic additives not as a substrate but as a mediator has helped raise the synthetic value of the reductive elimination of η^3-allylpalladium complexes.[3] Interestingly, the olefinic additives were shown to have no effect on the reductive elimination of dialkylpalladium complexes containing PR_3 ligands,[7b,13a] although the reaction of different dialkyl complexes, $PdR_2(bpy)$, was affected by olefins.[13b]

In the hope of attaining solutions to the problems described above, we have carried out more extensive synthetic and kinetic experiments of the reductive elimination of η^3-allylpalladium complexes. Emphasis has been laid on the independent confirmation of the reaction scheme derived from the kinetic studies. Then the work was further extended to detailed molecular orbital analysis based on the extended Hückel method. The new results of these studies are now described.

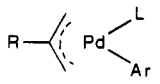

1

a: Ar = $C_6H_3Cl_2$-2,5; R = H; L = PPh_3
b: Ar = $C_6H_3Cl_2$-2,5; R = H; L = $P(C_6H_4Cl\text{-}4)_3$
c: Ar = $C_6H_3Cl_2$-2,5; R = H; L = $P(C_6H_4Me\text{-}4)_3$
d: Ar = $C_6H_3Cl_2$-2,5; R = H; L = $P(C_6H_4OMe\text{-}4)_3$
e: Ar = $C_6H_3Cl_2$-2,5; R = H; L = $P(OPh)_3$
f: Ar = $C_6H_3Cl_2$-2,5; R = H; L = $AsPh_3$
g: Ar = $C_6H_3Cl_2$-2,5; R = H; L = $As(C_6H_4Cl\text{-}4)_3$
h: Ar = $C_6H_3Cl_2$-2,5; R = H; L = $As(C_6H_4OMe\text{-}4)_3$
i: Ar = $C_6H_3Cl_2$-2,5; R = Me; L = PPh_3
j: Ar = C_6HCl_4-2,3,5,6; R = Me; L = $AsPh_3$
k: Ar = Ph; R = H; L = PPh_3

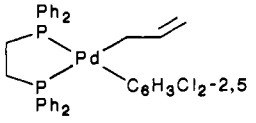

2

Results and Discussion

Spontaneous Reductive Elimination of 1 and 2.[14] Complexes **1a**, **1f–i**, and **1k** were prepared from the corresponding η^3-allylpalladium chlorides and ArZnCl. **1b–e** were formed in solutions in quantitative yields (by ^1H NMR) from **1f** and the appropriate L. The η^1-allyl complex **2** was prepared in a manner similar to that for the polyhaloaryl analogues.[16]

Complexes **1** underwent spontaneous decomposition in toluene under nitrogen at ≥0 °C (**1a–i**) or ≥−30 °C (**1k**) to give the coupling product (allylbenzenes). Stoichiometry of the reaction (eq 1) was very high (>90%) when **1** was decomposed in the

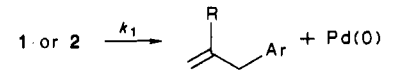

1 or 2 $\xrightarrow{k_1}$ + Pd(0) (1)

presence of a large excess of L ([L]/[**1**] ≥ 4).[17] Of particular relevance to mechanistic considerations is the fact that addition of L to a $CDCl_3$ or toluene-d_8 solution of **1** did not result in appearance of any ^1H NMR resonances assignable to new species. All that we could observe was broadening and coalescence of the syn-anti allyl proton resonances,[18] which may be ascribed to occurrence of eq 2.[10,16b] It should be stressed here that the η^1-allyl

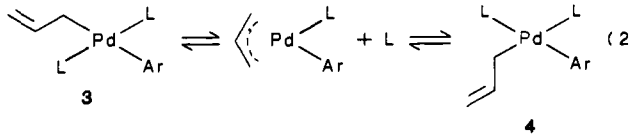

3 **4** (2)

species, **3** and **4**, are formed only transiently or their equilibrium concentrations are extremely low, as judged from almost no change of the allyl proton chemical shifts except for averaging of the coalescing protons' shifts.

In Table I are shown the rate constants for eq 1 determined in the presence of varying amounts of L. From Table I it is apparent that k_1 of eq 1 is not affected by the amount of L added. In Table II are summarized rates and activation parameters for various complexes in several solvents.

Table I. Rate Constants (k_1) for Equation 2 in the Presence of L[a]

complex	L	concn, M	$10k_1$, h^{-1}
1a	PPh_3	0.0570	2.12[b]
		0.120	2.11
		0.200	2.01
1e	$P(OPh)_3$	0.130	10.3
		0.260	9.98
1f	$AsPh_3$	0.0800	0.377[b]
		0.200	0.438

[a] In toluene at 30 °C. Initial concentrations of the complexes were 0.020 M. [b] Initial rate.

Table II. Kinetic Data[a] for Equation 2

complex	solvent	$10k_1$, h^{-1}	$\Delta H^{\ddagger}$, kJ mol^{-1}	$\Delta S^{\ddagger}$, J K^{-1} mol^{-1}
1a	toluene	2.08	95 ± 2	−14 ± 6
	$ClCH_2CH_2Cl$	1.24	99 ± 5	−5 ± 15
	MeCN/THF (5/3)[b]	0.954	99 ± 1	−8 ± 3
1b	toluene	4.39	90 ± 1	−24 ± 3
	acetone	2.00	92 ± 3	−22 ± 9
1c	toluene	0.887	101 ± 1	0 ± 3
1d	toluene	0.783	101 ± 1	0 ± 3
1e	toluene	10.1	93 ± 2	−6 ± 4
1f	toluene	0.408	105 ± 1	7 ± 3
1i	toluene	0.257	102 ± 2	−7 ± 7
2[c]	toluene	0.578	114 ± 3	27 ± 9

[a] At 30 °C. [b] By volume. [c] At 40 °C.

(10) Vrieze, K. *Dynamic Nuclear Magnetic Resonance Spectroscopy*; Jackman, L. M., Cotton, F. A., Eds.; Academic: New York, 1975; p 441.
(11) Numata, S.; Kurosawa, H. *J. Organomet. Chem.* **1977**, *131*, 301.
(12) Kurosawa, H.; Emoto, M.; Urabe, A.; Miki, K.; Kasai, N. *J. Am. Chem. Soc.* **1985**, *107*, 8253.
(13) (a) Komiya, S.; Akai, Y.; Tanaka, K.; Yamamoto, T.; Yamamoto, A. *Organometallics* **1985**, *4*, 1130. (b) Sustman, R.; Lau, J.; Zipp, M. *Tetrahedron Lett.* **1986**, *27*, 5207.
(14) A portion of this section (thermolysis of **1**) has been communicated in ref 15.
(15) Kurosawa, H.; Emoto, M. *Chem. Lett.* **1985**, 1161.
(16) (a) Numata, S.; Okawara, R.; Kurosawa, H. *Inorg. Chem.* **1977**, *16*, 1737. (b) Kurosawa, H.; Urabe, A.; Miki, K.; Kasai, N. *Organometallics* **1986**, *5*, 2002.
(17) Under these conditions the rate was first order with respect to [**1**] up to more than 2 half-lives. The first-order rate constants for **1b** in the presence of $P(C_6H_4Cl\text{-}4)_3$ (0.164 M) were independent of the initial concentrations of **1b** (0.01, 0.02, 0.04 M). Thermolysis in the absence of L afforded the allylbenzenes (ca. 30–50%) and low yields of biphenyl, benzene, or 1,4-dichlorobenzene, together with unidentified Pd complexes and Pd black.
(18) On adding $AsPh_3$ (As/Pd = 4) to **1f** at room temperature, all the allyl proton resonances became only broader. Addition of PPh_3 (P/Pd = 4) to **1a** at room temperature resulted in coalescence of the syn and anti protons cis to PPh_3 and broadening (with disappearance of ^{31}P coupling) of the syn and anti protons at the other site.

Table III. Rate Constants for Reactions of **1f–h** with Olefins[a]

complex	olefin	10^4k_2, h^{-1}	10^4k_3, M	k_2/k_3, M^{-1} h^{-1}
1f	CH_2=$CHCH_2Cl$	1.90 ± 0.30	1.37 ± 0.35	1.39 ± 0.57
	CH_2=$CHCH_2Br$	2.57 ± 0.19	0.75 ± 0.38	3.4 ± 2.0
	CH_2=$CHCH_2OAc$	1.45 ± 0.21	6.4 ± 1.3	0.227 ± 0.079
	CH_2=CHCN	24.3 ± 1.3		
	CH_2=CHCOOMe	45.4 ± 1.2		
	Z—MeOOCCH=CHCOOMe	150 ± 6		
	E—MeOOCCH=CHCOOMe	(2.51 ± 0.09) × 10^3		
	E—NCCH=CHCN	(4.78 ± 0.77) × 10^3	(1.02 ± 0.17) × 10^3	4.7 ± 1.5
1g	CH_2=$CHCH_2Cl$	7.81 ± 0.49	4.86 ± 0.74	1.61 ± 0.35
1h	CH_2=$CHCH_2Cl$	0.745 ± 0.054	0.88 ± 0.21	0.85 ± 0.26

[a] In toluene at 0 °C. For rate expression, see eq 4 and 5.

Thermolysis of **2** also afforded good yields of the coupling product, even though good first-order kinetics were observed up to only ca. 60% conversion. Again the rate was not affected by added dppe ligand. As shown in Table II, this reaction had considerably smaller rate constants and larger $\Delta H^{\ddagger}$ values than those for the reaction of **1**.

In the reaction of *cis*-$PdMe_2(PR_3)_2$, a reaction scheme involving reversible dissociation of PR_3 to form a T-shaped intermediate, followed by the C–C coupling step, was proposed[7a,b] and has received theoretical support.[7c] On the other hand, the results in Table I showing k_1 independent of the amount of L added may exclude the prior dissociation of L from **1**. These data also indicate that the second molecule of L is not involved in the rate-determining step, excluding the 5-coordinate intermediate Pd(η^3-allyl)(Ar)L_2 and the η^1-allyl intermediate **4**. As shown before, **4** exists only transiently. On the basis of the kinetic results of Table I solely, we cannot distinguish between the C–C coupling directly from **1** or from a 3-coordinate η^1-allyl intermediate **5**. At the moment we prefer the direct path in view of the kinetic parameters showing little solvent dependence (Table II), whereas these parameters for the dissociative reductive elimination of *cis*-$PdMe_2(PR_3)_2$ were remarkably solvent dependent.[7a] Further molecular orbital analysis of these processes will be given in a later section.

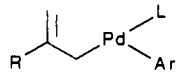

5

The rate data of Table II for **1a–d** indicate the lower reactivity of the complex having the better donating ligand, in agreement with the theoretical prediction.[7c] Of particular note in Table II is the lower reactivity of **1f** than of **1a–d**. The order of k_1 (PPh_3 > $AsPh_3$) is the same as that of the rate of H_2 elimination from $[IrH_2(CO)_2L_2]^+$.[19] Furthermore, oxidative addition of IrCl(CO)L_2 is more favored for L = $AsPh_3$ than for L = PPh_3.[20] These facts altogether appear to point to the notion that the stability of the PPh_3 complexes relative to that of the $AsPh_3$ complexes is increased more as the oxidation state of the metal atom becomes lower. This trend could be explained if we assume more π-accepting character for PPh_3 than for $AsPh_3$ and/or more σ-donating character for $AsPh_3$ than for PPh_3. Although the significance of π-interaction in the metal–phosphine bond remains controversial,[21] enhancement of the C–C coupling by coordination of a better π-acid[22] was manifested in the reaction of **1** with olefins, as described next.

Kinetics of Olefin-Promoted Reductive Elimination of 1. Addition of some olefins (e.g., fumaronitrile, allyl chloride) to a toluene solution of **1** resulted in rapid formation of the coupling product in high yields even at 0 °C for the dichlorophenyl analogues and −50 °C for the phenyl analogue. Stoichiometry of the reaction with allyl chloride is given in eq 3, where a very high yield of the η^3-allylpalladium chloride was confirmed by ^1H NMR spectra. The reaction of **1** with olefins other than allyl chloride would have given Pd(0) complexes whose composition is a function of the ratio of [olefin]/[L] employed. However, precise structure of such products was not determined.

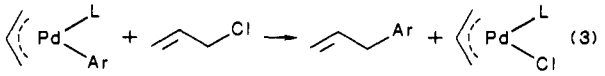

(3)

The acceleration of the reaction of **1** by the olefins was compensated for considerably by adding PPh_3 or $AsPh_3$. Because of the potential reactivity of PPh_3 with those olefins employed, kinetic measurements were made for the reaction of **1f** at 0 °C in the presence of varying amounts of $AsPh_3$.[23a] Fairly clean first-order dependence of [**1f**] was observed up to ca. 2 half-lives in the presence of rather low concentrations of $AsPh_3$ ([$AsPh_3$] = 2.2 × 10^{-4}–2.2 × 10^{-3} M) for the reaction of allyl chloride ([C_3H_5Cl] = 0.3–2.46 M) or high amounts of $AsPh_3$ ([$AsPh_3$] = 0.02–0.4 M) for the reactions of other olefins ([olefin] = 0.05–2.3 M).[23b]

From linear plots of k_{obsd} vs. [olefin] and $1/k_{obsd}$ vs. [$AsPh_3$] (see supplementary material), we found that the rate obeyed eq 4 for the reaction of allyl chloride and fumaronitrile. Similar results were obtained for the reaction of allyl bromide and acetate with **1f** and that of allyl chloride with **1g** and **1h**. For the reaction

$$\text{rate} = k_{obsd}[\mathbf{1}] = \{k_2[\text{olefin}]/(k_3 + [AsR_3])\}[\mathbf{1}] \quad (4)$$

of olefins other than allylic electrophiles and fumaronitrile, it was difficult to estimate meaningfully large intercepts in linear plots of $1/k_{obsd}$ vs. [$AsPh_3$] (see supplementary material). This leads to eq 5. Table III summarizes k_2 and k_3 values determined for several olefins.

$$\text{rate} = k_{obsd}[\mathbf{1}] = \{k_2[\text{olefin}]/[AsR_3]\}[\mathbf{1}] \quad (5)$$

Since no adduct formation occurs between **1f** and $AsPh_3$ as described before, we suggest the inverse dependence of the rate on [AsR_3] as due to dissociation of AsR_3 prior to the C–C coupling step. Consistent with eq 4 are Schemes I and II. In Scheme I a steady-state approximation is applied to the concentration of intermediate **6**, leading to $k_2 = k_4k_5/k_{-4}$ and $k_3 = k_5/k_{-4}$. Scheme II involves a rapid preequilibrium (eq 8) to form 3-coordinate intermediate **7**, followed by a slow reaction of **7** with the olefin to give the product, leading to $k_2 = k_6K_{diss}$ and $k_3 = K_{diss}$.

Scheme II can readily be excluded, since k_3 for the reaction of **1f** varies considerably as the olefin changes (Table III), while this scheme requires constant k_3 ($=K_{diss}$) values irrespective of the olefins. Moreover, Scheme II should yield constant k_2/k_3 ($=k_6$) values for a given olefin irrespective of the nature of AsR_3. However, this is not the case as shown by the increase of k_2/k_3 for the reaction of C_3H_5Cl in the order **1h < 1f < 1g** (Table III). This order is explained in terms of the ease of ligand exchange

(19) Mays, M. J.; Simpson, R. N. F.; Stefanini, F. P. *J. Chem. Soc. A* **1970**, 3000.
(20) Deeming, A. J.; Shaw, B. L. *J. Chem. Soc. A* **1969**, 1802.
(21) Reference 2a, p 54.
(22) The higher reactivity of **1e** than the others in Table II may be compatible with the greater π-accepting ability of $P(OPh)_3$ than PR_3.[21]

(23) (a) Half-lives of these kinetic runs never exceeded 70 h, which is sufficiently smaller than the half-life of spontaneous reductive elimination of **1f** at 0 °C (1700 h), estimated from data of Table II, as to eliminate the contribution of the latter process. (b) At the concentrations of $AsPh_3$ lower than those indicated, deviation from linearity of plots of ln [**1f**] vs. time was considerable from the very early stages of the reactions. Pseudo-first-order rate constants (k_{obsd}) were not dependent on the initial concentration of **1f** (0.005–0.05 M).

Scheme I

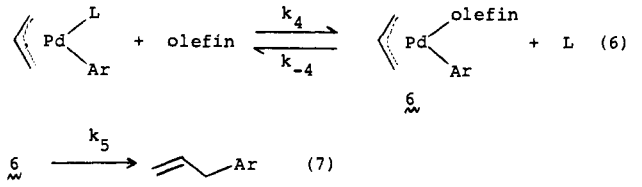

Scheme II

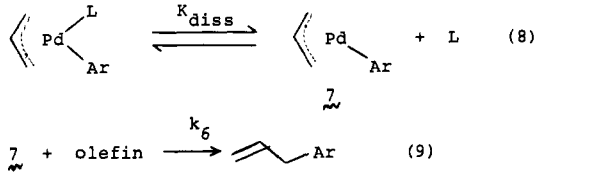

(eq 6) where $k_4 = k_2/k_3$. This explanation may also be applied to the change of k_3 ($=k_5/k_{-4}$) for C_3H_5Cl in the same order. Now Scheme I appears most appropriate for eq 4. Under the reaction conditions employed for obtaining eq 5, [$AsPh_3$] may well be sufficiently larger than k_3 ($=k_5/k_{-4}$ of Scheme I) to eliminate the latter term from eq 4.

The k_4k_5/k_{-4} ($=k_2$) value varies over a wide range among the olefins examined (Table III). On the other hand, the variation of k_4 ($=k_2/k_3$) that we could determine is much narrower.[24] These trends would be explained if we assume it is k_5 that strongly reflects the electrophilic nature of the olefin.[26] Less electrophilic olefins, typically styrene, did accelerate the reductive elimination of **1f**, but not remarkably enough to allow accurate determination of k_2 values. Of further note is that k_4/k_{-4} may well be so small[27] that k_5 for each olefin included in Table III would be much larger than k_2, and hence k_1 (4×10^{-4} h^{-1}) of **1f** at 0 °C which could be calculated by extrapolation. These assumptions will be confirmed by separate experiments in the next section.

It should be noted here that addition of strong electrophiles other than the olefinic substrates was not so effective in enhancing the C–C coupling of **1**, as exemplified by facile Pd–Ar bond cleavage by *N*-bromosuccinimide or Br_2.[16b] Metallic oxidants such as $IrCl_6^{2-}$ and $CuCl_2$ were also ineffective. Addition of fumaronitrile and allyl chloride to the η^1-allyl complex **2** caused no acceleration of the reductive elimination. Furthermore, maleic anhydride and **2** induced very rapid formation of propene, possibly via electron-transfer activation of the Pd–allyl bond.[16b]

Formation and Reductive Elimination of η^3-Allyl(aryl)(olefin)palladium. Attempted preparation of Pd(η^3-allyl)($C_6H_3Cl_2$)(olefin) by the reaction of [Pd(η^3-allyl)Cl]$_2$ with $C_6H_3Cl_2ZnCl$ in the presence of excess olefin (e.g., styrene) resulted in Pd metal deposition even at −50 °C. However, similar treatment of the chloride dimer/styrene mixture with Tl(C_6HCl_4-2,3,5,6)$_3$ at −60 °C resulted in almost quantitative formation of complex **8a** as deduced by ^1H NMR spectroscopy measured at −30 °C. This spectral assignment was unambiguously made by referring to the platinum analogue Pt(η^3-CH_2CMeCH_2)(C_6F_5)(styrene), which was isolated stable. The other substituted styrene complexes **8b–f** were identified similarly. Attempts to isolate **8a–f** in a pure state were unsuccessful. Dimethyl maleate complex **8g** was also confirmed unambiguously at −45 °C, although **8g** underwent reductive elimination rather rapidly even at this temperature (see below). Methyl acrylate and acrylonitrile complexes **8h** and **8i** were also formed at −60 °C, but their spectra were too complicated to be resolved well.

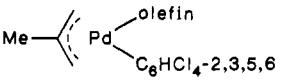

8

a: olefin = CH_2=CHC_6H_5
b: olefin = CH_2=CHC_6H_4OMe-4
c: olefin = CH_2=CHC_6H_4Me-4
d: olefin = CH_2=CHC_6H_4Cl-4
e: olefin = CH_2=$CHC_6H_4NO_2$-4
f: olefin = CH_2=$CHC_6H_4NO_2$-3
g: olefin = (*Z*)-MeOOCCH=CHCOOMe
h: olefin = CH_2=CHCOOMe
i: olefin = CH_2=CHCN

The ready coordination of olefins in **8** appears of particular relevance to the regiocontrolled steroid synthesis from a η^3-allylpalladium chloride dimer and organozirconium reagent.[3e] Key to the mechanism in this transformation is the coordination of olefinic ligands to the η^3-allylpalladium moieties. However, olefins do not usually form any complex with [Pd(η^3-allyl)Cl]$_2$,[28] including allyl = CH_2CMeCH_2 utilized in our experiment above, stable enough to be detected spectroscopically. Thus, formation of **8** may give strong credence to the proposed mechanism in the steroid synthesis.

The relative stability of substituted styrene complexes (eq 10) was determined by ^1H NMR spectroscopy at −30 °C. The equilibrium constants are shown in Table IV and a Hammett plot is given in Figure 1. The data indicate that the palladium atom in **8** is only very weakly electrophilic in nature toward olefin (Hammett $\rho = -0.25$, $r = 0.960$). This trend is in sharp contrast

Table IV. Equilibrium Constants (K_{eq}) for Equation 10[a]

Y	K_{eq}	Y	K_{eq}
4-OMe	1.2	4-NO_2	0.74
4-Me	1.2	3-NO_2	0.63
4-Cl	0.86		

[a] In $CDCl_3$ at −30 °C.

Table V. Rate Constants (k_7) for Equation 11[a]

complex	temp, °C	k_7, h^{-1}	complex	temp, °C	k_7, h^{-1}
8a	10	0.281[b,c]	**8f**	10	2.44[b]
8b	10	0.136[b]		−10	0.175
8c	10	0.221[b]	**8g**	−45	2.71[d]
8d	10	1.01[b]	**8h**	−10	1.23
8e	10	5.48[b]	**8i**	−10	2.56[e]

[a] In toluene; [**8**] = 0.05 M and [olefin] = 0.50 M except as noted. [b] Initial rate. [c] [Olefin] = 0.25, 0.50, and 1.0 M. [d] In $CDCl_3$. [e] [Olefin] = 0.50 and 1.0 M.

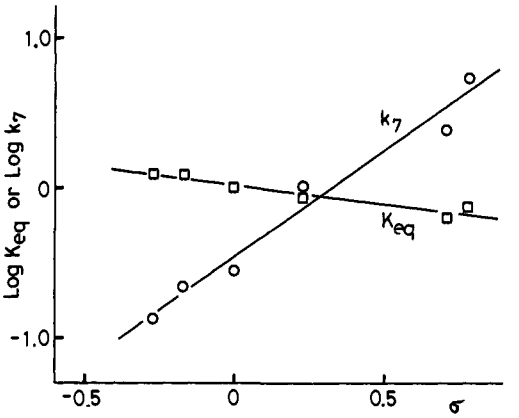

Figure 1. Hammett plots for K_{eq} (eq 10, □) and k_7 (eq 11, ○).

(24) The order of k_4 for the reaction of **1f** with CH_2=$CHCH_2X$ (X = Br > Cl > OAc), though narrow in the range, is similar to that of the apparent second-order rate constants for the reaction of **1a** with these allyl compounds.[25] However, the latter constants might not necessarily correspond to k_4 of eq 6, for the pseudo-first-order rate constants for the reaction of **1a** with CH_2=$CHCH_2X$ were measured without added PPh_3 and found to depend, unlike in the case of **1f**, on the initial concentration of **1a** used. It is possible that the reaction scheme for **1a** is somewhat different from that for **1f**.

(25) Kurosawa, H.; Emoto, M.; Urabe, A. *J. Chem. Soc., Chem. Commun.* **1984**, 968.

(26) Similar trends were observed in the reaction of dialkylnickel complexes with olefins.[8a]

(27) We could not detect the olefin-coordinated intermediate **6** by ^1H NMR spectra *during the reductive elimination* (Experimental; however, see the next section).

(28) Volger, H. C.; Vrieze, K.; Lemmers, S. W. F. M.; Praat, A. P.; van Leeuwen, P. W. N. M. *Inorg. Chim. Acta* **1970**, *4*, 435.

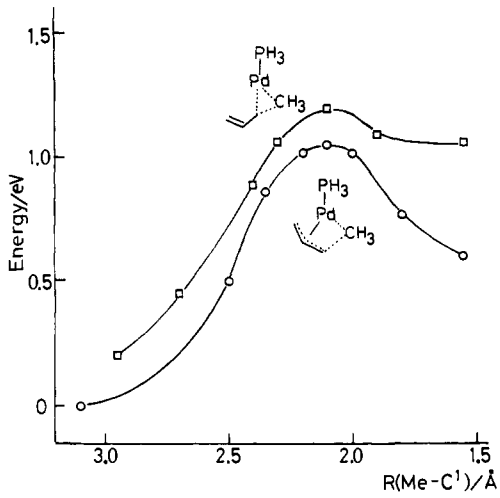

Figure 2. Total energy change along the hypothetical path for reductive elimination of **11a** (□) and **13a** (○).

to the much more electrophilic nature of Pd in other complex systems.[29]

$$Pd(CH_2{=}CHC_6H_5) + CH_2{=}CHC_6H_4Y \overset{K_{eq}}{\rightleftharpoons} Pd(CH_2{=}CHC_6H_4Y) + CH_2{=}CHC_6H_5$$

$$Pd = Pd(\eta^3\text{-}CH_2CMeCH_2)(C_6HCl_4\text{-}2,3,5,6) \qquad (10)$$

Complexes **8** underwent reductive elimination rapidly at higher temperatures to give relatively high yields (>80%) of the coupling product (eq 11). The rate was first order in the complex, even though kinetic behavior in the case of a series of styrene complexes was not very clean after ca. 1 half-life, presumably owing to lack of suitable ligands for stabilizing Pd(0) species; similar observations have been noted previously in both spontaneous and olefin-promoted reductive elimination of **1**. The rates of eq 11 for **8a** and **8i** were found to be independent of the amount of free olefin added (0.25–1.0 M; [**8**] = 0.05 M). The k_7 values determined for several olefins are shown in Table V. A Hammett plot for k_7 of substituted styrene complexes is shown in Figure 1. For comparison, the rate constants at 10, −10, and −45 °C for the reductive elimination of $Pd(\eta^3\text{-}CH_2CMeCH_2)(C_6HCl_4)(AsPh_3)$ (**1j**) were estimated as 1×10^{-6}, 2×10^{-8}, and 2.5×10^{-12} h^{-1}, respectively, by extrapolation with the activation parameters determined at much higher temperatures (Experimental Section). It now became quite evident that these values are by far smaller than k_7 in Table V.

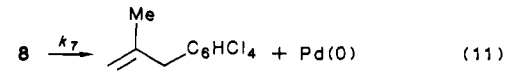

(11)

In a series of substituted styrene complexes, a complex containing the more electron-withdrawing olefin gives the larger k_7 value, with the ρ value of the Hammett equation being 1.42 (r = 0.983). This trend, together with other data in Table V, unambiguously confirms the suggestion described in the last section that the complex having the more electrophilic olefin reacts more rapidly. Furthermore, comparison of the two Hammett ρ values for eq 10 and 11 suggests a greater sensitivity of the rate constant (k_7) than of the equilibrium constant (K_{eq}) to the electronic factor of the olefin substituent. This is also in line with the rate data shown in Table III that are associated with Scheme I; namely, the variation of k_2/k_3 ($=k_4$) is narrower than that of k_2 ($= k_4k_5/k_{-4}$).

Molecular Orbital Analysis of Reductive Elimination of η³- and η¹-Allylpalladium Complexes. In order to gain a theoretical insight into reactivity patterns of the allylpalladium complexes, we simulated the three reaction pathways (Scheme III) based on the extended Hückel method. We first compare energetics of eq 12–14 for phosphine-coordinated models, **9a**, **11a**, and **13a**, and then examine effects of substituting ethylene for PH_3 (**9b**, **11b**, **13b**) on these reactions.

Scheme III

(L = PH_3 a; $CH_2{=}CH_2$ b)

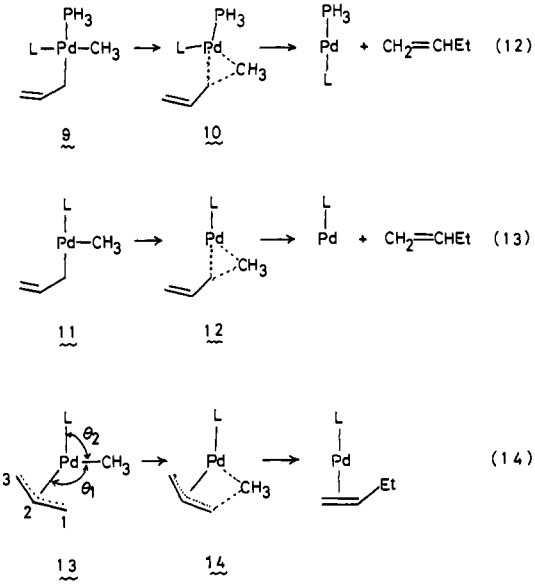

(i) η³-Allyl vs. η¹-Allyl Intermediate. Reductive elimination of η¹-allyl and CH_3 in eq 12 and 13 (L = PH_3) was simulated in a manner[30] similar to those reported for dimethylpalladium models, $Pd(CH_3)_2(PH_3)_2$ and $Pd(CH_3)_2(PH_3)$.[7c] We found the reaction of the four-coordinate complex **9a** meets a notably higher barrier (1.6 eV) than that of the three-coordinate complex **11a** (1.0 eV). This trend compares well with the different barriers of the ethane elimination from $Pd(CH_3)_2(PH_3)_2$ (1.7 eV) and $Pd(CH_3)_2(PH_3)$ (1.1 eV).[7c]

The coordination geometry of the η³-allyl in **13a** was set (see Appendix) by referring to some crystal structures of η³-allyl complexes of Pd and Pt containing the relevant ligand groups.[31,32] With the optimized angles of $\theta_1 = 125°$ and $\theta_2 = 105°$, we obtained the energy of **13a** as 0.20 eV lower than that of **11a**, in harmony with the observed geometrical preference. However, in view of our failure to observe, in ^1H NMR spectra of **1** at room

(29) (a) Kurosawa, H.; Majima, T.; Asada, N. *J. Am. Chem. Soc.* **1980**, *102*, 6996. (b) Ban, E.; Hughes, R. P.; Powel, J. *J. Organomet. Chem.* **1974**, *69*, 455.

(30) We varied the three geometrical parameters simultaneously in describing the reductive elimination of **9a** and **11a** as was done for the dimethyl models. These are the elongation of the Pd–C distances, the rocking motion of η¹-allyl and CH_3, α (see **15**), and the C–Pd–C angle. For the reaction of **9a**, the P–Pd–P angle was also changed at the same time. Due to steric interferences, the C=C part of **9** and **10** finds the minimum energy position at one rotameric form shown in **16** where the dihedral angle between Pd–C^1–C^2 and C^1–C^2–C^3 planes is around 90°. In **11** and **12**, the energy of **16** is almost the same as that of another rotamer in which C^2 and CH_3 are trans to each other.

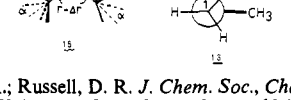

15 16

(31) (a) Mason, R.; Russell, D. R. *J. Chem. Soc., Chem. Commun.* **1966**, 26. (b) Mason, R.; Whimp, P. O. *J. Chem. Soc. A* **1969**, 2709. (c) Brock, C. P.; Attig, T. G. *J. Am. Chem. Soc.* **1980**, *102*, 1319. (d) Godleski, S. A.; Gundlack, K. B.; Ho, H. Y.; Keinan, E.; Frolow, F. *Organometallics* **1984**, *3*, 21. (e) Jolly, P. W. *Angew. Chem., Int. Ed. Engl.* **1985**, *24*, 283.

(32) (a) Miki, K.; Kai, Y.; Kasai, N.; Kurosawa, H. *J. Am. Chem. Soc.* **1983**, *105*, 2482. (b) Miki, K.; Yamatoya, K.; Kasai, N.; Kurosawa, H.; Emoto, M.; Urabe, A. *J. Chem. Soc., Chem. Commun.* **1984**, 1520. (c) Miki, K.; Yamatoya, K.; Kasai, N.; Kurosawa, H.; Emoto, M.; Urabe, A.; Tatsumi, K.; Nakamura, A., manuscript in preparation. (d) Miki, K.; Kasai, N.; Kurosawa, H., unpublished.

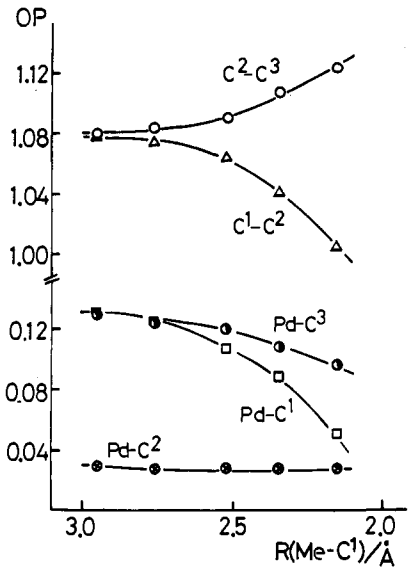

Figure 3. Overlap population change in reaction of **13a** as the function of Me–C^1 distance: C^1–C^2 (△); C^2–C^3 (○); Pd–C^1 (□); Pd–C^2 (⊗); Pd–C^3 (◑).

temperature, a *spontaneous* syn-anti allyl proton exchange which is expected to proceed through a $\pi \rightleftarrows \sigma$ rearrangement via an intermediate similar to **11a**, it may well be that our calculations somewhat underestimated the energy difference between **13a** and **11a**.

As for the simulation of the reaction pathway of eq 14, a full geometrical optimization for searching for the transition state **14a** appears too difficult to attain. Instead, we employed a simplified approach, by varying primarily the parameters shown in **13** and **17** (for details, see Appendix). The calculated energy curve along the model reaction coordinate is shown in Figure 2.[33] Also shown in this figure is the energy profile for the reaction of the three-coordinate η^1-allyl model **11a**.[33]

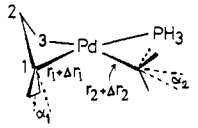

17

The potential energy curve for the reaction of **13a** indicates that the intramolecular rearrangement from a η^3-allyl(methyl) to a η^2-butene complex occurs smoothly, with a barrier of 1.05 eV. The aspect of the growth of the η^2-butene complex character in the course of the reaction may be illustrated in a somewhat simplified manner as shown in Figure 3.

In Figure 3 we compare the change of the C^1–C^2 and C^2–C^3 overlap populations as a function of the Me–C^1 distance, while keeping the C^1–C^2, C^2–C^3, Pd–Me, and Pd–C(allyl) distances unchanged from those of **13a**. It is apparent that two C–C bonds in the C^1–C^2–C^3 skeleton become progressively asymmetrical toward C^1—C^2=C^3 as the Me—C^1 bond is formed. Also shown in Figure 3 is the change of the Pd–C(allyl) overlap population. Interestingly, the Pd–C^2 and Pd–C^3 overlap populations are almost unchanged, so that the original Pd–C^2 and Pd–C^3 bond strengths are retained in the course of the reaction.

In Figure 2 we note that the energy maximum (**14a**) for eq 14 (L = PH_3) lies ca. 0.15 eV lower than that (**12a**) for eq 13 (L = PH_3). This agrees with our proposal concerning the relative ease of reductive elimination of **1** directly through the η^3-allyl form and through **5**. Furthermore, the lower barrier for eq 13 (L = PH_3) than for eq 12 (L = PH_3) agrees with the lack of coupling path from intermediate **4** discussed before.

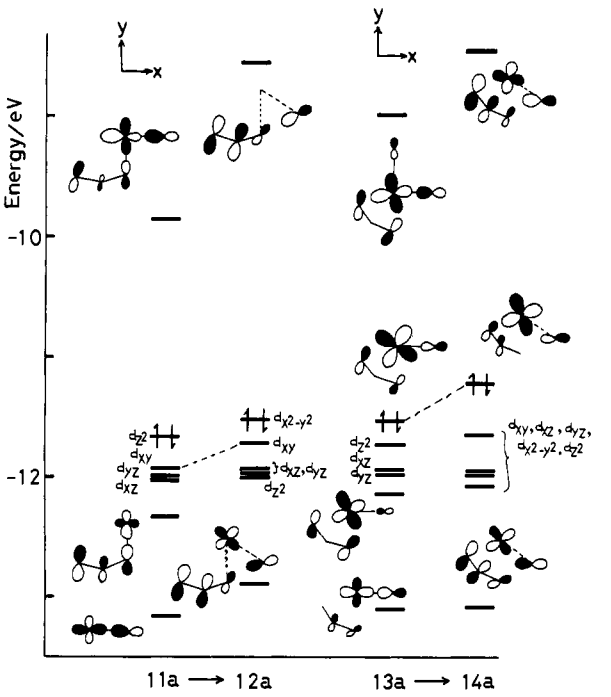

Figure 4. Orbital energy diagram for reactions of **11a** → **12a** and **13a** → **14a**.

The orbital diagram for the reaction of **11a** and **13a** is shown in Figure 4. It seems somewhat difficult to deduce the relative stability of **11a** vs. **13a** and **12a** vs. **14a** solely from this diagram. Nevertheless, the extra bond energy gained by the coordination of the C=C part of the allyl ligand to Pd may contribute to the overall stabilization of **13a** relative to **11a** and that of **14a** relative to **12a**. In this regard, retention of the Pd–C^2 and Pd–C^3 bond strength as is reflected in the overlap population change in Figure 3 in the reaction path of eq 14 seems instructive. Although the Me–C^1 overlap population is larger in **12a** (0.371) than in **14a** (0.321), the sum of Pd–C(allyl) and Pd–CH_3 overlaps in the latter (0.256) is sufficiently larger than that in the former (0.123) to overcome the Me–C^1 overlap disadvantage.

(ii) Effect of Olefin Coordination. In a manner quite analogous to those used for the PH_3-coordinated models, we calculated the potential energy curves for the reactions of ethylene-coordinated models, **9b**, **11b**, and **13b** (eq 12, 13, 14; L = CH_2=CH_2). It was found that only the reaction of the η^3-allyl complex, **13b**, gains a *lower* barrier than that of **13a** (by 0.12 eV), while those of **9b** and **11b** require a *higher* barrier than those of **9a** and **11a**, respectively (both by ca. 0.1 eV). We attribute these results as primarily due to stabilization of the transition state in the reaction of the η^3-allyl-(η^2-ethylene) complex as discussed below.

First we note that the energy of the transition state of the η^3-allyl-(η^2-ethylene) model **14b** lies ca. 0.36 eV lower than that of the η^1-allyl counterpart **12b**. This difference is considerably larger than that in the PH_3 complexes shown before (**14a** vs. **12a**; 0.15 eV). In contrast, on the reactant side the energy difference between the ethylene-coordinated η^3- and η^1-allyl models (**13b** vs. **11b**; 0.2 eV) is almost the same as that in the PH_3 case (**13a** vs. **11a**).

In order to look into the Pd–ethylene interaction in the η^3-allyl complexes, we made our calculations using the Pd(η^3-C_3H_5)(CH_3) fragments[34] of **13b** and **14b**. The fragment orbitals relevant to π interaction are shown in Figure 5. The figure exhibits a notable rise of the fragment orbital, which is suited for the π back-bonding with the π^* of in-plane coordinated ethylene on going from **13b**

(33) The energy maximum of **14a** corresponds to the structure having Pd–C^1 = 2.24 Å, Pd–C^2 = 2.15 Å, Pd–C^3 = 2.20 Å, Pd–CH_3 = 2.30 Å, C^1–CH_3 = 2.10 Å, C^1–C^2 = 1.50 Å, C^2–C^3 = 1.40 Å, $\alpha_1 = \alpha_2 = 40°$, θ_2 = 114°; the angle between the allyl and the coordination plane is 115°; C^2 lies 0.40 Å above the coordination plane. The other maximum of **12a** contains the geometries Pd–CH_3 = Pd–CH_2 = 2.30 Å, α = 55°, C–Pd–C = 36°, P–Pd–CH_3 = 126°.

(34) The reaction barrier for this hypothetical ligand free η^3-allyl model was almost the same as in eq 14 (L = PH_3).

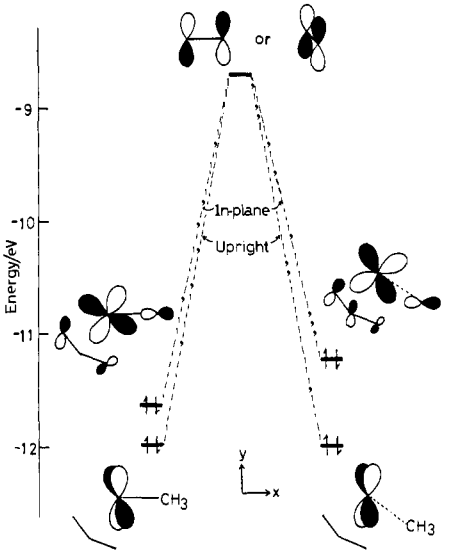

Figure 5. π back bond interaction in **13b** (left) and **14b** (right).

Table VI. Relative Energy and Overlap Population of In-plane and Upright Ethylene Complexes

	ΔE,[a] eV	OP[Pd–C(ethylene)][b] in-plane	upright
11b	0.17	0.307	0.314
12b	−0.09	0.321	0.305
13b	0.01	0.333	0.307
14b	−0.24	0.341	0.296

[a] $E_{Inp} - E_{Up}$. [b] Total Pd–C overlaps.

to **14b**, while the other orbital d_{yz}, suited for the π interaction with upright ethylene, remains constantly low. Thus, the more effective π back-bonding is expected in **14b** with the in-plane coordinated ethylene than in any other situation. This is indeed confirmed by the total energy and the Pd–C(ethylene) overlap populations in **13b** and **14b** with the in-plane and upright geometries, as summarized in Table VI. Also included in this table are the corresponding data for the η^1-allyl complexes, **11b** and **12b**.

We also calculated the orbitals of the η^1-allyl fragments, Pd(η^1-C_3H_5)(CH_3), and found that the energy levels of the d orbitals responsible for π interaction with ethylene in **11b** and **12b** are much the same as those of the corresponding d orbitals of **11a** and **12a** shown in Figure 4. Moreover, the latter two may in turn be regarded as the fragments for ethylene coordination in **9b** and **10b**.[35] In Figure 4 it is seen that on going from **11a** to **12a** d_{xy} of **11a** rises to only a small extent and d_{yz} and d_{xz} remain almost unchanged. Thus, in the transition state of the reaction of the η^1-allyl models (**10b**, **12b**) π back-bonding interaction is not expected to be strong enough to help stabilize the transition state (see Table VI). Rather, the strong donor character of the ethylene π orbital relative to PH_3 is probably a cause for the increased barrier in these reactions when compared to those in the PH_3 cases.

Concluding Remarks. In the reductive elimination of Pd(η^3-allyl)(Ar)L in the presence of free ligand L, the C–C bond formation proceeds without participation of the η^3- to η^1-allyl conversion as long as L is PPh_3 or less basic phosphines. Dissociation of L also is not significant during the C–C bond formation. When L is replaced by an olefin, it plays a role apparently specific to the η^3-allyl system in lowering the barrier to the C–C bond formation.

Experimental Section

Preparation of 1 and 2. In a typical procedure, *n*-BuLi (8.7 mmol) in hexane was added under dry nitrogen to a THF solution (30 cm^3) of 1,4-dichlorobenzene (1280 mg; 8.7 mmol) cooled at −78 °C. The mixture was stirred at this temperature for 1 h. Then a THF solution (30 cm^3) of $ZnCl_2$ (1180 mg; 8.7 mmol) was added, and the temperature was raised to −50 °C. A THF solution (65 cm^3) of Pd(η^3-C_3H_5)Cl(PPh_3) (1940 mg; 4.36 mmol) was added dropwise. After the mixture was stirred for 2 h, a MeOH solution of HCl (4.35 mmol) was added. The solvents were evaporated completely under vacuum while the temperature of the reaction vessel was maintained below 0 °C. The residual solids (pale yellow) were washed by cold methanol and water and dried under vacuum (yield of crude product, ca. 80%). They were recrystallized from benzene/*n*-hexane in a refrigerator (below −10 °C) to give almost colorless microcrystalline solids of **1a**. Similar procedures gave **1i** (colorless crystal) and **1f–h** (pale-red or red-brown crystals). **1j** and **2** were prepared in a manner similar to those reported for analogous complexes.[11,16] Melting point (with decomposition): **1a**, 88 °C; **1f**, 142–143 °C; **1g**, 89–90 °C; **1h**, 99–100 °C; **1i**, 120 °C; **1j**, 145 °C; **2**, 99–102 °C. These products gave satisfactory analytical results (C, H). Typical allyl proton ^{1}H NMR data (C_6D_6) (for proton numbering scheme, see the structure for **18**): **1a**, δ 2.57 (d, J_H = 13 Hz, H^1), 3.01 (dd, J_H = 12, J_P = 10 Hz, H^4), 3.51 (dd, J_H = 7 and 2.5 Hz, H^2), 3.93 (br t, J_H = J_P = 7 Hz, H^3), 5.09 (m, R); **1f**, δ 2.58 (d, J_H = 14 Hz, H^1), 2.96 (d, J_H = 14 Hz, H^4), 3.68 (dd, J_H = 7.5 and 2.5 Hz, H^2), 3.92 (br d, J_H = 7 Hz, H^3), 4.99 (m, R); **1i**, δ 1.67 (s, R), 2.57 (s, H^1), 2.88 (d, J_P = 9 Hz, H^4), 3.34 (d, J_H = 3 Hz, H^2), 3.76 (dd, J_P = 5 Hz, H^3); **2**, δ 2.95 (br m, $PdCH_2$), 4.45 (br d, J_H = 15 Hz, =C*H*H), 4.60 (br d, J_H = 10 Hz, =CH*H*), 6.29 (m, —CH=), 1.5–2.2 (m, PCH_2).

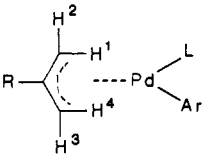

18

The phenyl analogue **1k** was prepared in a manner similar to that for **1a** from PhZnCl and Pd(η^3-C_3H_5)Cl(PPh_3) except that the reaction temperature was maintained at −70 °C, evaporation of the solvents was done at ca. −20 °C, and the recrystallization step was omitted. ^{1}H NMR ($CDCl_3$) at −30 °C: δ 2.78 (d, J_H = 13 Hz, H^1), 2.75 (t, J_H = J_P = 12 Hz, H^4), 3.53 (d, J_H = 7 Hz, H^2), 3.76 (br t, J_H = J_P = 7 Hz, H^3), 5.43 (m, R).

Identification of 8 by ^{1}H NMR Spectra. An NMR tube containing a deaerated $CDCl_3$ solution (0.1 cm^3) of [Pd(η^3-CH_2CMeCH_2)Cl]$_2$ (0.1 mmol) and appropriate olefin (0.2–1.0 mmol) was fitted with a serum cap and cooled to −60 °C. To this solution was added, drop by drop, a $CDCl_3$ solution (0.4 cm^3) of Tl(C_6HCl_4-2,3,5,6)$_3$[36] (0.1 mmol) with a hypodermic syringe to give rise to white precipitates of Tl(C_6HCl_4)$_2$Cl. After the solution was left to stand at this temperature for 0.5 h, the tube was placed in a probe kept at −45 or −30 °C. Spectra showed, within the detection limit, that all of the η^3-methallylpalladium chloride had reacted to form **8**. ^{1}H NMR ($CDCl_3$, see **18** where L = olefin): **8a** (major isomer), δ 1.35 (s, Me), 2.92 (s, H^4), 3.40 (s, H^1), 3.73 (s, H^3), 3.78 (s, H^2), 4.06 (d, J_H = 9 Hz, =C*H*H), 4.52 (d, J_H = 14 Hz, =CH*H*), 6.20 (dd, =CH–); **8a** (minor isomer) δ 1.83 (s, Me), 2.10 (s, H^1), 2.98 (s, H^4), 4.03 (d, J_H = 9 Hz, =C*H*H), 4.61 (d, J_H = 14 Hz, =CH*H*), 5.96 (dd, =CH—); **8g**, δ 1.98 (s, Me), 3.26 (s, H^4), 3.41 and 3.77 (s, OMe), 4.37 (br s, H^3), 4.71 (d, J_H = 10.5 Hz, —CH=), 4.92 (br s, H^2), 5.49 (d, =CH—), 7.26 (s, C_6HCl_4).

^{1}H NMR spectral data of **8b–f** are shown in Table S1. Equilibrium constants of eq 10 were determined by ^{1}H NMR spectroscopy in a manner quite similar to that reported[37] for analogous complexes, [Pt(η^3-CH_2CMeCH_2)(styrene)(PPh_3)]$^+$ and Pt(η^3-CH_2CMeCH_2)Cl(styrene).

Preparation of Pt(η^3-CH_2CMeCH_2)(C_6F_5)(CH_2=CHPh). To a THF solution (10 cm^3) of C_6F_5Li (0.15 mmol) and styrene (0.5 cm^3) kept at −78 °C was added Pt(η^3-CH_2CMeCH_2)Cl (0.1 mmol) in THF (8 cm^3). The mixture was warmed to −50 °C and kept at this temperature for 1 h. Methanol (0.2 cm^3) was added, and the solvents were evaporated under vacuum at ca. 0 °C. The residue was extracted with 3 × 10 cm^3 of benzene. After the solvent was evaporated under vacuum, the resulting solids were recrystallized from benzene–*n*-hexane to give colorless plates (40%): mp 97 °C; ^{1}H NMR ($CDCl_3$) major isomer, δ 1.40 (s, Me), 2.60

(35) The upright ethylene coordinated model gives considerably lower energy (by 1.6 eV for **9b** and 0.4 eV for **10b**) than the in-plane one possibly due to the steric origin; see: Albright, T. A.; Hoffmann, R.; Thibeault, J. C.; Thorn, D. L. *J. Am. Chem. Soc.* **1979**, *101*, 3801.

(36) Numata, S.; Kurosawa, H.; Okawara, R. *J. Organomet. Chem.* **1975**, *102*, 259.

(37) (a) Kurosawa, H.; Asada, N. *J. Organomet. Chem.* **1981**, *217*, 259. (b) Kurosawa, H.; Asada, N. *Organometallics* **1983**, *2*, 251.

(38) Hoffmann, R. *J. Chem. Phys.* **1963**, *39*, 1397.

Table VII. Extended Hückel Parameters

	orbital	H_{ii}, eV	exponent[a]
Pd	4d	−12.02	5.983 (0.5535) + 2.613 (0.6701)
	5s	−7.32	2.190
	5p	−3.75	2.152
P	3s	−18.6	1.60
	3p	−14.0	1.60
C	2s	−21.4	1.625
	2p	−11.4	1.625
H	1s	−13.6	1.3

[a] The d function is a double-ζ type.

(s, J_{Pt} = 61 Hz, H^4), 3.07 (s, J_{Pt} = 40 Hz, H^1), 3.67 (d, J_H = 9, J_{Pt} = 54 Hz, =C*H*H), 3.79 (s, H^3), 3.90 (d, J_H = 13.5, J_{Pt} = 54 Hz, =CH*H*), 4.02 (s, H^2), 5.95 (dd, J_{Pt} = 61 Hz, =CH—); ^{1}H NMR ($CDCl_3$) minor isomer, δ 1.89 (s, Me), 2.11 (s, J_{Pt} = 30 Hz; H^1), 2.52 (s, H^4), 4.32 (s, H^2), 5.32 (dd, J_H = 9, 13.5 Hz, =CH—). Anal. ($C_{18}H_{15}F_5Pt$) C, H.

Reductive Elimination of 1a–i and 2. Amounts of the coupling products 1-allyl-2,5-dichlorobenzenes formed by reductive elimination of **1a–i** and **2** were determined by GLC (SE-30, 3 mm × 2 m) analysis. Standard samples of these materials were prepared by reactions of ($C_6H_3Cl_2$-2,5)ZnCl (20 mmol) with CH_2=$CRCH_2Cl$ (R = H or Me) (25 mmol) in the presence of Pd(η^3-allyl)Cl (1 mmol) in THF (100 cm^3) at −30 °C for 5 h, followed by the usual workup and preparative GLC (SE-30). The compositions were confirmed by mass spectroscopy. Allyl proton ^{1}H NMR data (C_6D_6): CH_2=$CHCH_2C_6H_3Cl_2$, δ 3.10 (d, J_H = 6 Hz, $-CH_2-$), 4.76 (d, J_H = 16 Hz, =C*H*H), 4.81 (d, J_H = 9 Hz, =CH*H*), 5.53 (ddt, =CH—); CH_2=$CMeCH_2C_6H_3Cl_2$, δ 1.48 (s, Me), 3.12 (s, $-CH_2-$), 4.52 (s, =C*H*H), 4.72 (s, =CH*H*).

For a kinetic run of spontaneous reductive elimination, a test tube containing weighed amounts of complex (0.02–0.04 mmol) and L was fitted with a serum cap and filled with nitrogen gas. A nitrogen-saturated solvent (1–2 cm^3) and dodecane (GLC internal reference) were added at 0 °C with hypodermic syringes. The tube was immersed in a constant-temperature water bath. At appropriate intervals an aliquot (ca. 0.04 cm^3) was withdrawn by a syringe and poured into an acetone solution (0.04 cm^3) of HCl (ca. 5 equiv per Pd initially weighed) to quench unreacted **1**. The resulting solution was analyzed by GLC. The rate data determined in some solvents at different temperatures are summarized in Table S2.

Kinetic runs for olefin-promoted reductive elimination of **1f–h** were carried out similarly except that the reaction was triggered by adding appropriate amounts of olefins (or solutions of (*E*)-NCCH=CHCN and (*E*)-MeOOCCH=CHCOOMe) by a hypodermic syringe to a toluene solution of **1f–h** and AsR_3 at 0 °C. The rate data at several concentrations of olefins and AsR_3 are summarized in Table S3. For the reactions of allylic electrophiles and fumaronitrile, k_2 and k_3 were calculated by least-squares analysis of data ($1/k_{obsd}$ vs. [AsR_3]) at a given [olefin]. k_2 was also calculated from the relation between k_{obsd} and [olefin] at a given [AsR_3] by use of k_3 determined above.

Stoichiometry of some of the olefin-promoted reductive elimination was also confirmed by ^{1}H NMR spectroscopy in toluene-d_8 solutions. No resonances other than those of **1f**, CH_2=$CHCH_2C_6H_3Cl_2$-2,5, and the substrate olefin could be detected. We further tried to examine ^{1}H NMR spectra of reaction systems in which eq 6 was thought to have reached an equilibrium stage. For example, we presumed, on the basis of the order (ca. 1 M^{-1} h^{-1}) of k_4 which is rather insensitive to the nature of olefin, that 1 M of olefin substrate is enough to compel the forward path of eq 6 almost into completion in 10 h. At the same time formation of the coupling product could be suppressed to a very small extent within such duration by proper choice of [$AsPh_3$] (e.g., 0.2 M in the case of CH_2=CHCN). However, under these conditions we could not detect any resonance attributable to reaction intermediates.

Reductive Elimination of 1j and 8. Reductive elimination of **1j** in toluene-d_8 was followed by ^{1}H NMR spectroscopy in the same manner as that described before for analogous complexes.[11] The first-order rate constants thus determined are 3.47 h^{-1} (120 °C), 0.520 h^{-1} (100 °C), and 0.145 h^{-1} (90 °C); $\Delta H^{\ddagger}$ = 121 kJ/mol (100 °C); and $\Delta S^{\ddagger}$ = 3 J/(K·mol) (100 °C). The reactions of **8** were also followed by ^{1}H NMR and by GLC methods. For a kinetic run by GLC, a toluene solution (2 cm^3) of an olefin complex (0.1 mmol) and pentadecane (GLC internal reference) was prepared in a test tube at −60 °C by the method described before for the NMR measurement. The subsequent procedures were the same as those described above for the reaction of **1a–i** and **2** except that the method of quenching the reaction employed an acetone solution of dppe (5-fold excess) followed by addition of HCl.

Instruments. The following instruments were used: a JEOL PS-100 spectrometer (^{1}H NMR), a Hitachi RMU-6Z mass spectrometer (Mass), and a Hitachi 164 chromatograph (GLC).

Acknowledgment. Partial support of this work by a Grant-in-aid for Special Project Research, Ministry of Education, Science and Culture (61225016), is gratefully acknowledged.

Appendix

The parameters of the extended Hückel calculations[38] are listed in Table VII. A weighted H_{ij} formula was used for calculations. Geometrical assumptions included the following; η^3-allyl of **13**, Pd–C^1 = Pd–C^3 = 2.21 Å, Pd–C^2 = 2.17 Å, C^1–C^2 = C^2–C^3 = 1.40 Å, C^1–C^2–C^3 = 120°; the angle between the allyl and the coordination planes is 115°; terminal allyl hydrogens are bent back by 10°; other ligands, C–H = 1.09 Å, C–C = 1.50 Å, C=C(free) = 1.35 Å, C=C(coordinated) = 1.40 Å, P–H = 1.42 Å, Pd–C(sp^3) = 2.10 Å, Pd–C(olefin) = 2.15 Å, Pd–P = 2.30 Å, CH_3, $-CH_2-$, and PH_3 tetrahedral, C(sp^2) trigonal planar, ethylene hydrogens bent back by 10°.

The simulation of eq 14 was done as follows. At the early stages of the reaction, we kept the coordination geometry of the η^3-allyl group nearly unchanged from that in **13**; unchanged were the coordinates of C^2 and C^3, the C^1–C^2–C^3 angle, and the angle between the allyl and the coordination planes, while the C^1–C^2 distance was set as either 1.40 or 1.50 Å, and accordingly the Pd–C^1 distance as either 2.21 or 2.24 Å. With such η^3-allyl–metal frameworks fixed, we changed the Me–C^1 distance by varying the Pd-Me distance and θ_1, with θ_2, α_1, and α_2 (see **17**) being optimized for a given Me–C^1 distance. At later stages of the reaction we increased Δr_1 and Δr_2 and decreased θ_1 simultaneously, but we maintained the Pd–C^2 and Pd–C^3 distances at nearly 2.2–2.15 Å, so as to attain the final product Pd(η^2-but-1-ene)(PH_3) in which the Pd–C(olefin) distance was set as 2.15 Å. The C^1–C^2 and C^2–C^3 distances were fixed at 1.50 and 1.40 Å, respectively. The other parameters α_1, α_2, and θ_2 were varied for optimization.

Supplementary Material Available: Tables of ^{1}H NMR spectral and kinetic data, and figures for kinetic treatment (11 pages). Ordering information is given on any current masthead page.